ABSTRACT QUESTIONNAIRE

Please, fill out all fields of this questionnaire (except that corresponding to the Organizing Committee) and send by e-mail to the Symposium Secretariat as the front page of your abstract file in PDF format

ABSTRACT REF*.: _____

***For use only of the Organizing Committee**

Title:	Degradation of a Lithium Iron Phosphate based Cathode in Lithium-ion Batteries after 2000 cycles				
Presenting author:	Carmen M. Rangel	**Under 30 y.o.?**	No	**Presentation in English?**	Yes

EXPECTED CLASSIFICATION: (please, mark all the options that better define the research performed)

	MAIN SESSION
	PEM fuel cells
	SO fuel cells
	Other fuel cells
X	Batteries
	Supercapacitors
	Hydrogen
	Other

	SUB-CLASSIFICATION
	Numerical simulation
	New materials
	New processes
	Prototipe development
	Engineering & Integration
	Industrial project
	Marketing analysis
	Standards and regulations

Degradation of a Lithium Iron Phosphate based Cathode in Lithium-ion Batteries after 2000 cycles

M. J. Plancha[1], C.M. Rangel[1*], B. Rodrigues[2], F. Azevedo[2]

[1] *LNEG, Unidade de Pilhas de Combustível e Hidrogénio,Paço do Lumiar 22, 1649-038 Lisboa, (Portugal)*
[2] *A.A. Silva, S.A.-Autosil, Edif. Komax, E N 249-4, Trajouce, 2785-034 S. Domingos de Rana (Portugal)*

(*) corresponding author: mjoao.plancha@lneg.pt; carmen.rangel@lneg.pt

Keywords: Lithium-ion batteries, Lithium Iron Phosphate, Cathode degradation

1 Introduction

Lithium-ion batteries, first introduced by Sony in 1991 [1], have come to invade the market to replace Ni-Cd and Ni-MH batteries, particularly in applications such as portable telephones, computers and other devices, which usually utilize rechargeable batteries. World production of Li batteries came to 500 million units in 2000, and is believed to have reached 4.6 billion in 2010 [2].

Besides consumer electronics, the use of lithium ion-batteries is rapidly increasing in the automotive, aerospace and defense sectors due to its energy density. Next generation cars are likely to be powered by a combination of batteries, fuel cells and capacitors in hybrid system configurations that allow battery charging. No energy storage device by itself actually satisfies the demands of automotive applications [3].

Apart from the high energy density achieved, other major advantages of using Li-ion batteries are the low rate of self-discharge and excellent charge/discharge life cycles. The Li-ion cell has twice the capacity of Ni-Cd for the same volume and the discharge capabilities of the cell are better than that of Ni-MH, permitting higher current peaks. In addition, these batteries are environmentally acceptable. Whatever the technology used in its manufacture, the performance characteristics are related to the intrinsic properties of the electrode's materials.

The useful life cycles of charge/discharge and the total lifetime of the batteries (mentioned cycles and in rest period), are dependent on the nature of the interfaces between the electrodes and electrolyte, while safety is a function of stability of materials electrode and interfaces. The optimal combination of the group electrode-electrolyte-electrode can only be achieved through selective use of existing and new materials for the positive and negative electrodes, and the proper combination with the electrolyte, so as to minimize adverse reactions related to the interface electrode-electrolyte (critical phase of any electrochemical system).

In lithium-ion batteries, since the anode material is carbon, not containing lithium, the positive electrode (cathode) must act as a source of ions of this metal, thus requiring intercalation compounds based on lithium, stable in air, in order to facilitate the cell assembly. The most common cathode materials are lithium cobalt oxides ($LiCoO_2$), lithium nickel oxides ($LiNiO_2$), lithium manganese oxides such as $LiMnO_2$ and $LiMn_2O_4$, etc. In Table 1 some characteristics of cathode materials for lithium-ion batteries are depicted.

Lithium iron phosphate with an ordered olivine-type structure, belongs to a general class of "polyanion" compounds containing compact tetrahedral "anion" structural units $(XO_4)^{n-}$ (X = P, S, As, Mo or W) with strong covalent bonding in the lattice, to produce higher coordination sites such as oxygen octahedra that are occupied by other metal ions.

Other phosphates of lithium and transition metal such as Mn, Ni or Co have also been the subject of studies due to their high theoretical specific capacity ($170mAhg^{-1}$) [4]. However, $LiFePO_4$ is the most attractive due to its high stability, low cost and high compatibility with the environment (low toxicity). This compound has also a high lithium intercalation voltage (~ 3.5V vs. Li) and is easily synthesised [5].

Despite all these advantages, the full capacity of $LiFePO_4$ is difficult to be achieved, since its electronic conductivity is very low [6], which leads to initial capacity loss and to slow diffusion of Li^+ ion in the olivine structure [7]. Only at a very low current [8] or at elevated temperature [9] this material could achieve the theoretical capacity. $LiFePO_4$ electrodes are actually composed of two separate phases, $LiFePO_4$ and $FePO_4$, which are both poor electronic conductors because they each contain Fe cations with just one oxidation state (2+ or 3+, respectively).

In practice one could not obtain the full capacity of the material because, as the electrochemical reaction proceeds, 'electronically' isolated areas remain inactive in the bulk electrode. At a lattice scale, mixed electronic and ionic conductivity is required to preserve the neutrality of the total charge during the lithium-ion transport, being the chemical diffusion coefficient rate-limited by the slowest species.

Table 1 - Characteristics of cathode materials in lithium-ion batteries.

Electrode material	Nominal voltage (V)	Life cycles number	Specific charge* (Ah/Kg)
$LiCoO_2$	3.7	400	137
$LiMn_2O_4$	3.7	800	148
$LiFePO_4$	3.2	2000	170

* Theoretical

The selective doping of $LiFePO_4$ by multivalent cations such as Al^{3+}, Nb^{5+} and Zr^{4+} was first made at the Massachusetts Institute of Technology, by Chiang and colleagues, which showed that the electronic conductivity of lithium iron phosphate has increased 10 million times in relation to the conductivity of the undoped material, reaching up to 10^{-2} Scm^{-1} at room temperature [10]. The electronic conductivities obtained are far superior to other commonly used cathodes such as $LiCoO_2$ (~ 10^{-3} Scm^{-1}) and $LiMn_2O_4$ ($2x10^{-5}$ to $5x10^{-5}$ Scm^{-1}). The resulting doped $LiFePO_4$ materials have storage capabilities that are close to the theoretical limit of 170 $mAhg^{-1}$ at low charge/discharge rates.
In this paper, the degradation of Li-ion battery cathodes based on $LiFePO_4$ was evaluated by means of a post-mortem analysis done to a battery sample in the end of life and comparing it with the results obtained in a fresh cathode sample in the charged condition (without any charge/discharge cycle). The failure analysis was conducted by using SEM (Scanning Electron Microscopy) coupled with EDS (Energy Dispersion Spectroscopy) and X-ray diffraction on samples selected from the cathodes of batteries before and after charge/discharge cycles.

2 Experimental

Commercial Li-ion batteries with nominal voltage of 3.2V, having a graphite type negative electrode and a cathode based in lithium iron phosphate were subjected to ~2000 charge/discharge cycles in order to obtain an end-of-life condition.

A series of four batteries were first discharged at 20A during 1 hour (constant current protocol). Afterwards, continuous cycles of charge/discharge were performed with a time interval of 5 minutes between each charge and discharge step. The charges were done at a current density of 10A and a maximum voltage of 14.5V for 3 hours under constant current-constant voltage (CC-CV) condition. The part of the cycle corresponding to the discharge of the batteries was carried out at the same conditions of the first one. Cycled and fresh (in charged state) cylindrical Li-ion batteries were manually dismantled in a fume-hood.

After removal of the steel case at atmospheric pressure, the batteries were left to stand for 1 h in a vacuum system. The samples were then manually fully disassembled (unrolled) in an Ar filled glovebox, allowing recognition and separation of the components (cathodes, anodes, plastic cases, steel cases, copper foils, polymer foils and electrical contacts).

The analyses of cathode samples before and after charge/discharge cycles were done by using Scanning Electron Microscopy (SEM), coupled with Energy Dispersion Spectroscopy (EDS) using a Phillips XL 30 Model FEG scanning electron microscope at 2kV (to minimize charging of the uncoated samples), equipped with an energy dispersive X-ray detector.

X-Ray Diffraction (XRD) measurements were also carried out, using a Rigaku model D/Max III C automated diffractometer with graphite monochromated Cu radiation. Data were collected in the 2□ range from 5 to 105º at a scan rate of $1.2ºmin^{-1}$.

3 Results and Discussion

3.1 Battery cycling

Charge/discharge cycles were performed for a series of four batteries. Typical results for one complete cycle after the discharge of the batteries is shown in figure 1.

The voltage variation profiles obtained by constant current discharge and charge steps are shown, together with the current profile during the potentiostatic charge (constant voltage polarisation). As expected, the voltage value of the battery system decreases during the discharge (till about 10.5V in the first and second discharges observed in the figure) and increases during the galvanostatic charge. In this step, when voltage value reaches 14.5V, the switch to constant voltage charge (at 14.5V) is done.

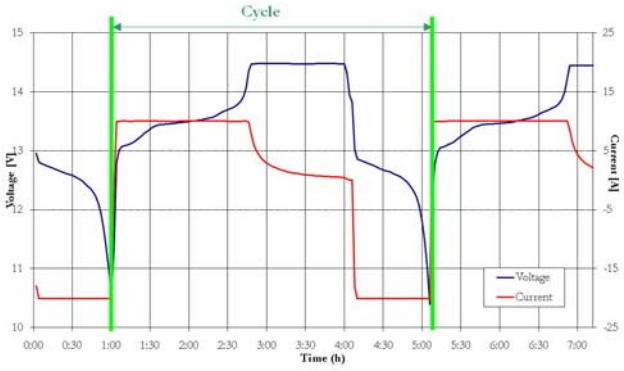

Fig. 1 Voltage and current variations with time in the charge/discharge cycling of the Li-ion based batteries used in this work. The graph shows data for four batteries connected in series.

3.2 SEM and EDS analyses

In order to observe morphological changes associated to the positive electrode and also to detect any eventual elemental composition change, SEM/EDS analyses were carried out on samples taken from a fresh and a cycled battery cathode.

SEM micrographs of the samples obtained at a magnification of 5000 X are shown in figures 2 and 3 respectively. It can be seen the presence of crystal aggregates together with the presence of some binder.

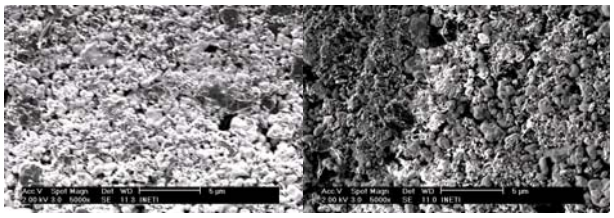

(a) (b)

Fig. 2 SEM micrograph of the fresh (in charged condition) (a) and cycled (b) cathode samples.

The aggregates are formed by microparticles with irregular shape and various sizes (typically 0.5 to 1µm and some with ~2µm), which assure a high specific area, and micropores, which allow the diffusion of the electrolyte to inner regions of the electrode. The battery cycled sample (Fig. 2b) shows some changes in morphology.

After the cycles, the amount of micropores seems to increase and to enlarge; simultaneously, the quantity of microparticles decreases. This may be indicative of an area decrease of the regions where the insertion/deinsertion takes place, bringing as a consequence a decrease of the battery capacity.

The results of EDS analyses made to the cathode's samples (Fig. 3) are consistent with the fact that the cathode of the Li-ion battery is based on a lithium iron phosphate, with zirconium metal ions as dopant, making it a compound of general formula $LiFe_xZr_{1-x}P_yO_z$.

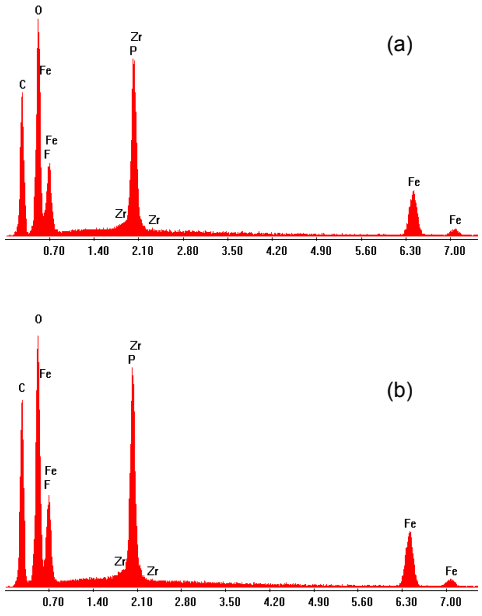

Fig. 3 EDS spectra correspondent to area analyses of sample shown in fig. 2: fresh (a) and cycled (b).

3.3 XRD analyses

X-ray diffraction analysis was employed to evaluate the crystal structure of the cathodes and identify any structural or crystalline composition changes with the cycling.

Figure 4 shows the X-ray diffraction pattern for the sample of the fresh cathode. The overall pattern (with the presence of various sharp peaks) indicates a relatively high degree of crystallinity. Diffraction peaks were identified as belonging to two crystalline compounds: iron phosphate, $FePO_4$ [11] and lithium iron phosphate, $LiFePO_4$ - "triphylite" [12]. This compound has an orthorhombic olivine-type structure with the oxygen atoms arranged in a slightly distorted, hexagonal close-packed arrangement [13]. The phosphorous atoms occupy tetrahedral sites, while the lithium and iron atoms occupy octahedral sites. The FeO_6-octahedra are linked through common corners in the *bc*-plane and the LiO_6-octahedra form edge-sharing chains in the *b*-direction. One FeO_6-octahedron has common edges with two LiO_6-octahedra. PO_4-groups share one edge with an FeO_6-octahedron and two edges with LiO_6-octahedra. The presence of the phase $FePO_4$ is representative of the partial conversion of $LiFePO_4$ to $FePO_4$. The diffraction pattern shows also a peak, marked "C" in figure 4, which belongs to graphite. This compound is part of the Li-ion battery composite cathode. The two phosphate phases found in the cathode, have also been refered in the study by Andersson and Thomas, as being present in the $LiFePO_4$ cathode of a lithium-ion battery after suffering one charge (up to 4.1V) [14].The existence of ion Zr^{4+} within the structure of lithium and iron phosphate can not be confirmed by this method since the X-ray diffraction pattern does not change with the introduction of small amounts of dopants, as shown in figure 5, from a published research work where cations such as Nb^{5+}, Ti^{4+}, Zr^{4+}, Al^{3+} and Mg^{2+} were introduced in samples of Li and Fe phosphate [10].

In figure 6 is presented the XRD pattern for the sample corresponding to the cycled cathode battery.Similarly, the cathode battery after charge/discharge cycles presents a high crystallinity degree. It appears that no distinct structural modification exists as no change in peak position is observed when comparing with the fresh sample. It is noted, however, an increase in the proportion between the intensity values of the iron phosphate characteristic peaks and those of the $LiFePO_4$ peaks for the cycled cathode, comparatively to the same diffraction peaks proportion of the fresh cathode. This might be indicative that the amount of lithium iron phosphate has decreased. Also, in the cycle discharge steps the intercalation of lithium turns sluggish with time and the conversion of $FePO_4$ for the lithiated form is only partially accomplished affecting the capacity of the battery.

Another structural study of $LiFePO_4$ at various rate and temperature conditions, made by *in situ* X-ray diffraction and *in situ* Raman spectroscopy,

also showed this conversion between the two phases of the cathode material, linked to the insertion and deinsertion processes of the lithium ion, on the lithium-ion battery cathode [15].

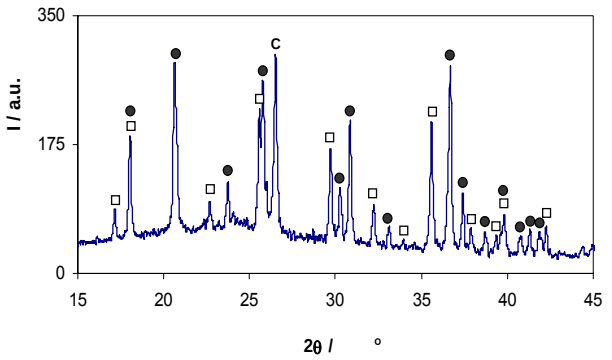

Fig. 4 X-ray diffraction pattern for the fresh cathode sample of the Li-ion battery under study. Compounds identified are: $FePO_4$ (●); $LiFePO_4$ (□).

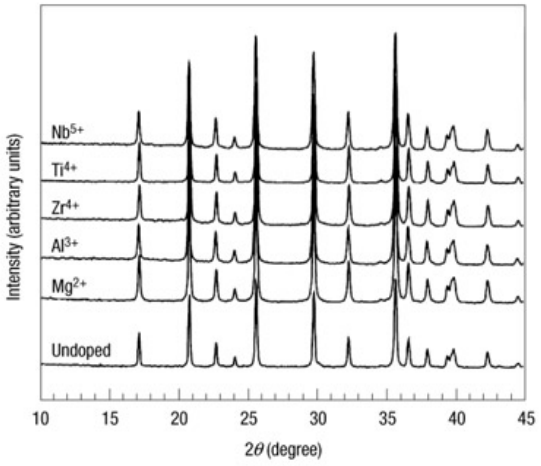

Fig. 5 X-ray diffraction patterns of several powders treated at 600 °C containing 1% (atomic percentage) of dopant, M, in the $Li_{1-x}M_xFePO_4$ stoichiometry.

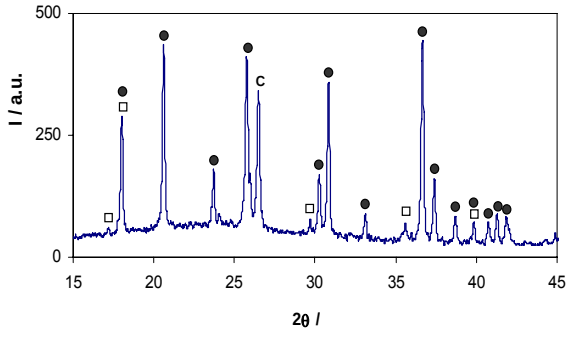

Fig. 6 X-ray diffraction pattern for the cycled cathode sample of the Li-ion battery under study. Compounds identified are: $FePO_4$ (●); $LiFePO_4$ (□).

4 Final remarks

Cathode EDS analysis is consistent with a cathode composition based on lithium iron phosphate.

The cathode is doped, for higher conductivity, with zirconium metal ions, making the battery's positive electrode mainly consisting in a compound of general formula $LiFe_xZr_{1-x}P_yO_z$.

The cathode is shown to have been modified with the imposed charge/discharge cycles. Changes were observed either in the morphology, either in the proportion of the existing crystalline compounds, the iron phosphate and the lithium iron phosphate.

The cathode microparticles regions decreased with the battery cycling indicating degradation of the electrochemical active area of the cathode.

Battery capacity also decreases as the conversion of $FePO_4$ to the lithiated form is only partially achieved in the discharge cycle step.

5 References

[1] M.B.J.G. Freitas, E.M. Garcia, J. Power Sources 171, pp 953, 2007.
[2] UMICORE, Materials Technology Group, http://www.umicore.com.
[3] Garry Golden, "Hydrogen storage could support lithium ion batteries in electric vehicles", 2008, http://www.theenergyroadmap.com.
[4] A.K. Padhi, K.S. Nanjundaswamy, J.B. Goodnough, J. Electrochem. Soc. 144, pp 1188, 1997.
[5] J. Chen, M.J. Vacchio, S. Wang, N. Chernova, P.Y. Zavalij, M.S. Whittingham, Solid State Ionics 178, pp 1676, 2008.
[6] A.S. Andersson, B. Kalska, L. Häggström, J.O. Thomas, Solid State Ionics 130, pp 41, 2000.
[7] B. Jin, H.-B. Gu, Solid State Ionics 178, pp 107, 2008.
[8] A. Yamada, S.C. Chung, K. Hinokuma, J. Electrochem. Soc. 148, pp A224, 2001.
[9] A.S. Andersson, J.O. Thomas, B. Kalska, L. Häggström, Electrochem. Solid-State Lett. 3, pp 66, 2000.
[10] S.-Y. Chung, J.T. Bloking, Y.-M. Chiang, Nature Materials 1, pp 123, 2002.
[11] JCPDS Card no 70-6685 (Powder Diffraction File, International Center for Diffraction Data, Swarthmore, PA).
[12] JCPDS Card no 81-1173 (Powder Diffraction File, International Center for Diffraction Data, Swarthmore, PA).
[13] V.A. Streltsov, E.L. Belokoneva, V.G. Tsirelson, N. Hansen, Acta Cryst. B49, pp 147, 2003.
[14] A.S. Andersson, O. Thomas, J. Power Sources 97-98, pp 498, 2001.
[15] K.Y. Chung, W.-S. Yoon, J. McBreen, X.-Q. Yang, K. Zaghib, H.C. Shin, C. S. Kim, W. I. Cho, B.W. Cho, in: 210th Meeting of The Electrochemical Society, Meet. Abstr., MA2006-02 / B3 - Lithium-Ion Batteries, Abstract #279, Cancun, 2006.